Journal of the Korean Chemical Society
2004, *Vol. 48, No. 4*
Printed in the Republic of Korea

시간 분해능 전자회절 분광법을 이용한 $CClF_3$분자의 평형 구조 연구

Seong S. Seo* and John D. Ewbank[†]
Department of Natural Science, Albany State University, Albany, GA 31705, USA
[†]*Department of Chemistry and Biochemistry, University of Arkansas, Fayetteville, AR 72701, USA*
(2004. 4. 21 접수)

Equilibrium Structure for $CClF_3$ Using Real-Time and Time-Resolved Gas Electron Diffraction

Seong S. Seo* and John D. Ewbank[†]
Department of Natural Science, Albany State University, Albany, GA 31705, USA
[†]*Department of Chemistry and Biochemistry, University of Arkansas, Fayetteville, AR 72701, USA*
(Received April 21, 2004)

요 약. 피코초 시간분해능 전자 회절 분광법(TRED)을 이용하여 $CClF_3$ 분자의 평형 구조를 연구하였다. 이 분광법의 분해능은 전자파의 선폭에 의하여 결정된다. 본 연구 방법에 의하여 결정된 $CClF_3$ 분자의 결합 길이들을 고전적인 실시간 전자회절 분광법(GED/RT)에 의하여 보고된 결과들과 비교하였다. GED/RT 방법에 의하여 결정된 C-F 결합 길이와 C-Cl 결합 길이는 각각 132.00(2) pm, 175.20(3) pm이고, TRED 방법에 의하여 결정된 C-F, C-Cl 결합 길이는 각각 132.23(13) pm, 177.23(19) pm 로써 이 두 실험 방법에 의하여 결정된 분자 결합 길이는 좋은 일치성을 보여준다.

주제어: 분자 구조, 시간분해능 전자회절 분광법, 기체 전자회절 분광법

ABSTRACT. The simplified cumulant method was applied to diffraction data of $CClF_3$ to study the equilibrium molecular parameters over a range of temperatures. The molecular parameters of $CClF_3$ by the simplified cumulant method were compared with those from the traditional method. Also the instrumentation of picosecond time resolved electron diffraction (TRED) and the experimental details are described. The total experimental temporal resolution was discussed in terms of the electron pulse width. The TRED system was applied to study the molecular structures for $CClF_3$ at room temperature. The molecular structural parameters $CClF_3$ from TRED are compared with those from GED/RT. The molecular parameters (r_e)of bonded C-F and C-Cl for $CClF_3$ by simplified CA are 132.00(2) pm and 175.20(3) pm, respectively, by using GED/RT. From the results of TRED experiments r_a for bonded C-F and C-Cl are 132.23(13) pm and 177.23(19) pm.

Keywords: Molecular Structure, Time-Resolved Electron Diffraction, Gas Electron Diffraction

INTRODUCTION

A real time gas electron diffraction (GED/RT)[1,2] instrument was constructed with a multichannel photodiode array (PDA) detector, and is thus an online technique. GED/RT has been applied to discriminate among various molecular force fields as derived from high-resolution spectroscopy. In conjunction with cumulant analysis,[3-5] the method determines not only the vibrational average structures, but also the equilibrium molecular geometries. The method applies to both equilibrium and non-equilibrium molecular ensembles. A simplified-CA (cumulant analysis) procedure[6] was developed recently to allow for data refinements without the need for extraneous information from spectroscopy.

To capture the dynamics of structures in transition states, ultrafast time resolution must be introduced to the diffraction. Previously, it was possible to probe such changes with femtosecond and picosecond spectroscopy to reveal the elementary nuclear motion.[7] The use of an ultrafast laser beams at the scattering center of GED/RT in order to photoexcite the molecules, and at the photocathode to make ultrashort electron pulses, provides a similar pump-and-probe process.

The first time resolved electron diffraction (TRED) system was used to study the structure of radical products formed in the IR multi-photon dissociation of CF_3I in the microsecond time domain.[8] The temporal resolution was further improved to nanoseconds (ns) by combining a laser initiated electron source with a linear diode array detector to study the 193 nm photodissociation of CS_2 in the time interval from 20-120 ns after excitation.[9] Recently, a TRED system has been reported to observe the UV-dissociation of CF_3I with picosecond (ps) time resolution.[7] Also, the photodissociations of Fe $(CO)_5$ and CF_2I_2 were studied with picosecond time resolution[10], but a clear result has not yet been attained. In recent years a number of other dynamic methods such as Time of Flight (TOF) mass spectroscopy and Femtosecond Transition-state Spectroscopy (FTS), have probed chemical reactivity in attempts to ascertain critical reactive intermediates and kinetic pathways.[7]

On the theoretical side, time-dependent equations for diffraction intensities have been derived for non equilibrium vibrational distributions for the case of photodissociated CS_2[11] and for the photoinduced coherent intramolecular dynamics of dissociative and predissociative transient states of ICN, IBr and NaI.[11] Also a new approach was developed to measure directly the quantum state of a molecular ensemble.[12] Only very recently TRED has become available as a new and complementary source of "structural kinetic" information for excited state species. In addition, the simplified-CA method was applied to the diffraction data of $CClF_3$. The TRED system was used to determine molecular structures for $CClF_3$. The molecular structural parameters $CClF_3$ from TRED are compared with those from GED/RT.

Theoretical Procedures

There exist alternative methods for calculating $I_{mol}(s)$ by making the vibrational and rotational averages, $\langle \exp[\, i\, \mathbf{s}(\mathbf{r}_i - \mathbf{r}_j)] \rangle$.[13] Displacements of the nuclear positions with respect to their equilibrium positions are expanded in terms of the normal coordinates and vibrational averages taken; then, the average over random orientations of the molecule is obtained. One can get reduced molecular intensities with cumulant average and the vibrational probability density function as follows [14]

$$sM(s) = \Sigma\Sigma_{i,j=1,N}\, g_{ij}(s)\, \exp\,[Q_{ij}(s)]/r_{e,ij}\{A_{ij}(s)\, \sin\,[s(r_{e,ij} + P_{ij}(s))] + B_{ij}(s)\, \cos\,[s(r_{e,ij} + P_{ij}(s))]\} \qquad (1)$$

where (omitting the subscripts ij for simplicity)

$Q(s) = -\, s^2 \langle \Delta r^2 \rangle_e / 2 + s^4 \langle \Delta r^4 \rangle_e / 24$

$P(s) = \langle \Delta r \rangle - s^2 \langle \Delta r^3 \rangle_e / 6$

$A(s) = 1 - [\langle \Delta r \rangle - s^2 \langle \Delta r^3 \rangle_e / 2] / r_e + \ldots$

$B(s) = [-\, s \langle \Delta r^2 \rangle_e + s^3 \langle \Delta r^4 \rangle_e / 6] / r_e + \ldots$

Equation (1) provides a basis for least-squares model refinement from GED data. One can adjust the equilibrium internuclear distances r_e and cumulants $\langle \Delta r^n \rangle_e$ with n = 1~4. The latter can be assigned a clear meaning in terms of properties determining the vibrational probability density function: $\langle r \rangle = r_e + \langle \Delta r \rangle$ is the mean position, $\langle \Delta r^2 \rangle_e = l_g^2$ is the dispersion, $\langle \Delta r^3 \rangle_e$ is the skew, and $\langle \Delta r^4 \rangle_e$ is the excess, respectively, of the probability density.

It is useful to consider the dimensionless cumulant coefficients, g_n, which are defined [15] by

$$\gamma_n = \langle \Delta r^n \rangle_e / \langle \Delta r^2 \rangle_e^{n/2} \quad n = 1, 3, 4, \ldots \qquad (2)$$

The g_n values are sensitive functions of the molecular force field and vibrational distribution. By inserting Eq. (2) into Eq. (1) one obtains

$$sM(s) = \Sigma\Sigma_{i,j=1,N}\, g_{ij}(s)\, \exp\,[Q_{ij}(s)]/r_{e,ij}\{A_{ij}(s)\, \sin\,[s(r_{e,ij} + P_{ij}(s))] + B_{ij}(s)\, \cos\,[s(r_{e,ij} + P_{ij}(s))]\} \qquad (3)$$

where,

$Q_{ij}(s) = -\, s^2 \langle \Delta r^2 \rangle_e / 2 + s^4\, g_4 \langle \Delta r^2 \rangle_e^2 / 24$

$P_{ij}(s) = g_i < \Delta r^2 >_c^{1/2} - s^2 g_i < \Delta r^2 >_c^{3/2} / 6$

$A_{ij}(s) = 1 - [g_i < \Delta r^2 >_c^{1/2} - s^2 g_i < \Delta r^2 >_c^{3/2} / 2] / r_e + \ldots$

$B_{ij}(s) = [- s < \Delta r^2 >_c + s^3 g_i < \Delta r^2 >_c^2 / 6] / r_e + \ldots$

To summarize, the cumulant method establishes a general relationship between diffraction intensity and cumulant averages defined with regard to the $P_{ij}(r)$ or $P_{ij}(r)/r$ functions. This relationship is accurate to any desired degree of approximation. The CA equation is based on geometrically consistent r_e parameters and is valid for non-equilibrium systems without extraneous information on harmonic and anharmonic potential constants. The traditional intensity equation is based on r_a geometries which are geometrically inconsistent. The molecular parameters obtained by cumulant analysis are more precise than those obtained by the traditional method. Further, the method may be applied to check the validity of anharmonic force fields derived from various spectroscopic investigations.

The simplified version of the CA of GED intensities was developed some time ago. In actual refinements of r_e and γ_{ij} from GED data, extensive parameter correlations were found.[15] Therefore, some approximate constraints between the cumulant coefficients are needed to apply Eq. (3) to GED data analyses without auxiliary spectroscopic calculations.

The least square refinements of molecular intensities can be performed on the basis of Eq. (3) with the approximate constraints. This is the scheme known as simplified CA. This simplified CA retains the conceptual consistency of full CA but allows for GED data refinements without the need for extraneous information or additional computational analysis. The simplified CA procedure can be applied to molecular ensembles at high temperatures and to excited systems. However, the omission of information on vibrational populations and potential constants in the simplified CA procedure is expected somewhat to diminish the accuracy in comparison to the full formalism.

In order to derive theoretical intensity expressions for non-equilibrium systems, one may use the theory afforded by cumulant expansions of the diffraction intensities. This level can be applied in studies of intramolecular vibrational redistribution processes at low levels of vibrational excitation, when the normal mode description of the molecular vibrations is still adequate. The processes of relating the harmonic and anharmonic force constants to electron diffraction intensities and spectroscopic constants are quite involved. First of all, the renormalized frequencies are calculated at the appropriate temperatures. Then, curvilinear internal coordinates are transformed to normal coordinates by a nonlinear transformatiom. Next the moments are calculated in terms of the potential function in normal coordinate space. Then the cumulants are calculated in internal coordinates and the molecular intensity function is obtained. The refinements are carried out with a Hooke and Jeeves computer algorithm.[16]

Instrumentation and Experimental Procedures of GED/RT and TRED

A) Instrumentation and Procedures for GED/RT

The GED/RT system has been described elsewhere.[1,2,17,18] There are three chambers (diffraction, electron and detector) with molecular inlet system and temperature controller. The diffraction and electron chambers are separated from each other and pumped independently. The electron chamber provides a stable high vacuum region for the collimation and positioning of the electron beam. The collimated electron beam interacts with the molecular beam in the diffraction chamber. A PDA is used for on line detection of the diffraction pattern on a fluorescent screen in the detector chamber.

The electron beam with well-defined wavelength is produced in an electron gun with a hot cathode filament of tungsten. The electrons are emitted thermally and are drawn and accelerated by the potential of the anode. The accelerated electrons leave the electron gun through a central hole in the anode. The electron beam is focused onto the registration plane by a magnetic lens.

Most groups still use densitometers which are single channel measuring devices to analyze the electron diffraction data. The method has proven to be successful but the stepping procedure is some-

what time consuming and, like all mechanical processes, it involves inevitable positioning uncertainties. Therefore, a position sensitive multichannel analyzer (PDA) is applied for analyses of the full diffraction pattern in one measurement. The PDA provides precise spatial resolution and offers high sensitivity and a large dynamic range. In the GED/RT instrument, a focused electron beam is crossed by a molecular jet, and the diffraction pattern is displayed on a fluorescent screen. The screen is optically coupled to a photodiode array which records the intensity distribution on-line, in a multichannel mode, and without the intervention of the rotating mechanical sector needed in photographic GED. The diffracted electrons are transformed into photons by the aluminized P20-type phosphor. The PDA is aligned on the opening of the butterfly slit. The PDA consists of a set of 1024 independent silicon photodiodes of pixel size 25 μm by 2.5 mm. The intensity distribution of the diffraction pattern with s range (50~280 nm^{-1}) is obtained and stored in digital form for immediate analysis. The real-time procedure allows for direct comparison of the scattered electron distributions from different substances.

Exposure time is usually 6 seconds at a PDA temperature of -30°C. Row data output can be viewed immediately on an oscilloscope, or more highly processed data can be displayed on the computer system monitor. Experimental variables such as the conditions of electron beam and scan state are maintained as constant as possible, and only the sample gas under study is changed. Gold thin film is used for alignment and focusing of the GED /RT system and N_2 is used for calibration purposes. For these studies a sample of $CClF_3$ (99.0%) was obtained from Aldrich and the purity checked with FT-IR.

CF_3Cl were studied under consistent experimental conditions at various temperatures. Instrumental variables such as electron accelerating voltage, scattering distance, sample temperature, detector temperature, and scan state were maintained as nearly constant as possible, and only the sample under study was changed. Argon gas yields a smooth intensity profile which is used to correct for slit unevenness, for nonuniformity of response of individual diode channels, and for other constant instrumental imperfections. N_2 gas is used for calibration of the electron diffraction instrument.

For an ideal GED apparatus, the total experimental scattered intensity of a molecule I^E_{tot} (s) is represented as the sum of an atomic background, I^E_{at} (s) and a contribution I^E_{mol} (s) from its internuclear distances. I^E_{ar} (s), the experimental intensity of argon, consists only of the featureless background type scattering. For two substances I and J, one defines the experimental ratio of their scattered intensities to be [19]

$$R^E_{IJ} = (I^E_{tot} - D) / (J^E_{tot} - D) \quad (1)$$

where D is the detector dark current or PDA signal when no sample gas is entering the diffraction chamber, but the main electron beam is present. The theoretical ratio is $R^T_{IJ} = I^T_{tot} / J^T_{tot}$ where $I^T_{tot} = I^T_{at} + I^T_{mol} + I^T_{tria}$, and the symbols have their usual meanings. I^T_{at} is the atomic scattering, I^T_{mol} is the molecular interference, and I^T_{tria} is the triatomic contribu-tion. One method of extracting the experimental molecular information is to apply the inverse atomic background ratio, $B^T_{JI} = J^T_{at} / I^T_{at}$ to the experimental data. In case the theoretical function J is monatomic, one obtains $B^T_{JI} R^T_{IJ} = 1 + M^T_I(s) + T^T_I(s)$ where $M^T_I(s)$ is the leveled molecular intensity. Similarly, when the theoretical inverse background ratio is applied to the experimental data, then

$$B^T_{JI} R^E_{IJ} = K(s) + R [M^E_I(s)] \quad (2)$$

where K(s) is a smooth function of the scattering variable s and R is an amplitude scaling constant which may be identified with the index of resolution. The K(s) and R values are determined that best fit the reduced experimental data to the current theoretical model. Eq. (2) is equivalent with the conventional M(s) curve of GED suited for structural analysis. Least-squares analyses are performed on the sM(s) functions of both the traditional and CA

methods until a self-consistent view of the experimental intensities and their theoretical counterparts are obtained. The molecular parameters (r_a, λ_a) for the traditional method and the molecular parameters (r_e, λ_e, γ_1, γ_3 and γ_5) for CA are obtained over the temperature range from 298K to 673K. As a parameter of accuracy of theoretical fit to the experimental GED data one uses a reduced reproducibility factor R_f defined as an integral standard deviation over the whole s-range between experimental and theoretical sM(s). The radial distribution (RD) curve shows maxima of radial probability which correspond to the internuclear distances.

B) Experimental Apparatus for TRED

The TRED apparatus is shown schematically in *Fig.* 1 for picosecond TRED. In *Fig.* 1 the optical pump laser pulses are directed to the diffraction chamber to excite the molecular sample. The probe laser pulses enter the electron chamber to generate picosecond electron pulses. The time delay between the pump and the electron pulses is controlled by a translation stage. The diffraction patterns are recorded with the electronic detection system. The following sections describe the individual components of picosecond TRED.

B. 1) Femtosecond Laser System

The laser system is divided into excimer pump laser, femtosecond laser[20], and excimer amplifier. The excimer pump laser (LEXTRA 100, Lambda Physik) is filled with premix XeCl (80mJ, 15ns pulses at 308 nm). The pump energy is distributed among the various dye cells of the femtosecond laser by quartz plates. The energy of the femtosecond system (Lambda Physik, FAMP/LEXtra) including amplified spontaneous emission (ASE) after the second amplifier was 250 μJ at 496 nm with 500fs pulse duration. The second harmonic generation in a BBO crystal provided the energy of 10-12 μJ at 248 nm, as measured by a Molectron J4 joulemeter. Also, the wavelength was measured with an Acton Research Corporation, SpectroPro-300I spectrometer.

The amplification of femtosecond pulses was accomplished by a slightly modified excimer laser (Questek). This laser was originally an oscillator with a 20 ns pulse of 100 mJ at 248 nm. The oscillator was converted to an amplifier by replacing the rear resonator mirror with a window. The amplifier

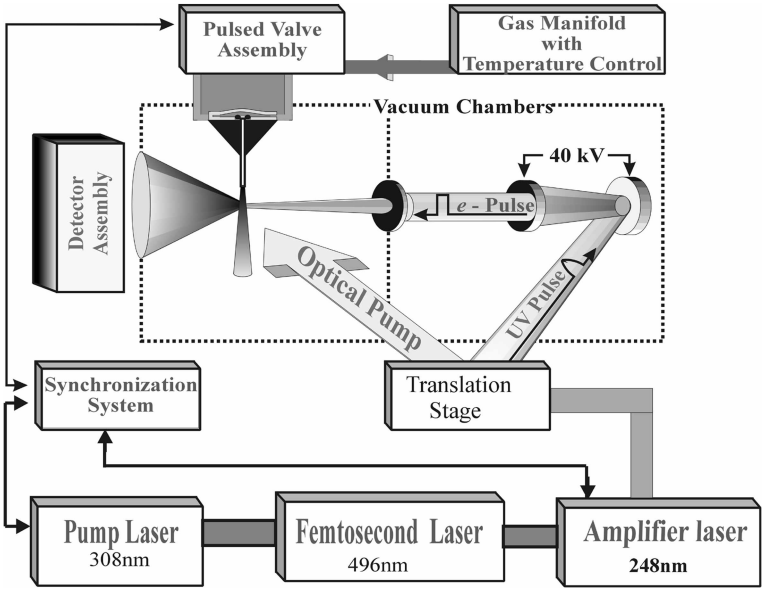

Fig. 1. The Schematic Diagram of the Picosecond TRED.

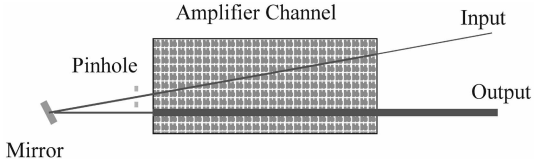

Fig. 2. Experimental Arrangement for Amplification of Femtosecond Laser Pulses.

was filled with a mixture of 150 mbar F_2, 150mbar Kr and remainder He to give a total pressure of 2700 mbar. After the first pass, the beam was filtered by a pinhole as shown in *Fig.* 2, and then sent through the amplifier a second time. By this double-pass amplification scheme, the pulse energy at 248 nm, 500fs was boosted to 3.5 mJ with no more than 7% amplified spontaneous emission (ASE).

B. 2) Electron Beam

The electron gun consists of two electrodes, a magnetic lens and diaphragms as shown in *Fig.* 3. The cathode is a circular tantalum (Ta) disk within a pierce-type electron gun.[21] The emitted electrons are accelerated through a potential of 40 keV. The picosecond electron pulses are reduced to a width of less then 2 mm at the intersection with the molecular beam. The ultrafast electron pulses travel to the diffraction center over a distance of about 50 cm.

The total temporal resolution (t_{TOT}) of an ultrafast electron pulse depends on the duration of the initial energy spread of the photoelectrons (Δt_{TD}), the coulombic dispersion of the electron pulse (Δt_{CI}) due to local space charge (LSC) during its time of flight, the duration of the laser pulse (Δt_{LP}), and a geometry factor (Δt_{GF}), as shown in *Fig.* 3. Therefore

$$(\Delta t_{TOT})^2 = (\Delta t_{GF})^2 + (\Delta t_{TD})^2 + (\Delta t_{CI})^2 + (\Delta t_{LP})^2$$

The geometric effect (Δ3ps) on the duration of the picosecond electron pulse is calculated by (w/c)tan(α_p), where w = 2 mm is the diameter of the laser beam at the photocathode, $\alpha_p = 40^\circ$ is the illumination angle for the laser beam, and c is the speed of light. The broadening of the pulse due to the initial energy spread is ~0.5ps. When electrons are ejected, the electron pulses traveled to the detector with collimation and focusing. After the moment of generation, electron-electron coulombic repulsion causes additional temporal broadening (Δt_{CI}). We estimate this space-charge temporal broadening is ~4-15 ps. The last term (Δt_{LP}) corresponds to the temporal duration of the laser pulse which creates the photoelectrons. As mentioned earlier, Δt_{LP}~0.5ps. Thus the overall electron pulse duration is in the range Δt_{TOT} = ~8-19ps.

B. 3) Pulsed Inlet System

TRED consists of two vacuum chambers. The electron chamber is maintained at a vacuum of 10^{-6} torr and the diffraction chamber at 10^{-4}-10^{-6} torr. The vacuum is maintained by two diffusion pumps (Edwards Models 160 and 63 Diffstaks) backed by two mechanical pumps (Edwards Model E2M40 and Varian SD 300, respectively).

We have used a modified commercial (Jordan)

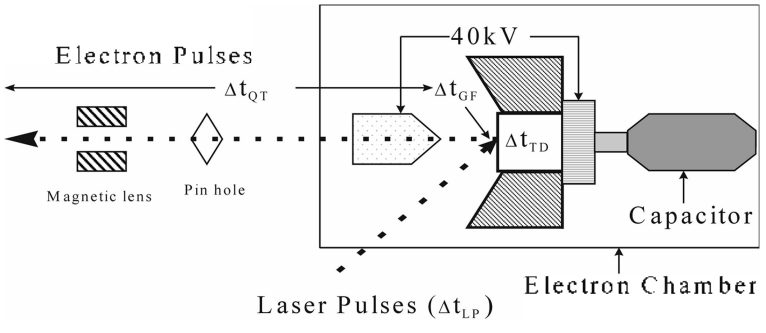

Fig. 3. The Schematic Diagram of the Electron Chamber and the Temporal Broadening Factors in the Formation of Picosecond Electron Pulses.

supersonic molecular beam pulsed valve (PV) inlet to maximize the scattering intensities for picosecond TRED. The PV consists of a hairpin loop of highly conductive metal[22] and is clamped on both ends with a hole in the bottom plate. A Viton O-ring is placed at the inside of the hole, and sealed by the upper plate. The magnetic repulsion generated by the opposing currents pushes the flexible upper plate away from the O-ring seal and allows gas to flow through the O-ring. The general pulse duration determined by the mechanical response of the upper plate is 30 to 100 ms depending on the pressure and drive current. The maximum repetition rate is 12Hz. The PV can operate at a maximum 10 atm pressure and about 100°C. The output orifice (d = 0.5 mm) of the free jet is extended with a cylindrical channel formed by a stainless hypodermic needle of length 25 mm and inside diameter 0.5 mm to achieve higher molecular densities in the scattering region.

B. 4) Data Acquisition System

The schematic diagram of the data acquisition system[23] is shown in *Fig.* 4. The diffraction patterns are recorded through an aluminized P-20 phosphor screen coated onto the surface of a vacuum tight fiberoptics faceplate. The phosphor screen is mounted on a standard 10-inch stainless steel flange that provides enough room to place a trap for the main electron beam. The butterfly is used to avoid the over saturation of the signal at small scattering angles and to compensate for signal fall off at larger angles. Furthermore, a linear neutral density filter was designed on the opposite end of the fiber optic coupler. The intensity angular range was nearly equalized with the EF but the signals were still weak for the picosecond experiment. Two fiber optic couplers (Schott) were used for the data acquisition system. The fiber optic couplers consist of a core glass (n = 1.6) and an outside tube of cladding glass which has a lower index of refraction (n = 1.4). Integration over a longer exposure time was previously used to compensate for weak signals but the dark noise became unacceptably large. The use of a microchannel plate (MCP) intensifier (ITL Ltd, MCP-140) has provided good results with shorter exposure times. A microchannel plate (MCP) is an array of 10^4-10^7 miniature electron multipliers oriented parallel to one another; typical channel diameters are in the range 10-100 μm. Channel multipliers typically operate at gains of 10^3-10^5. The photodiode array (PDA) (RY-2048 diode array, Princeton Instruments) detector consists of 2048 side-by-side elements having pixel dimensions of 25 μm x 2.5 mm. All the diodes in the array are read out after a single integration period and the spectral data stored in the computer memory for display. The CSMA (Princeton Instruments) is a complete control and data collection system. The cooling of the system is essential to reduce the dark current of the PDA. After the system is turned on, it usually takes about two hours for the thermoelectrically

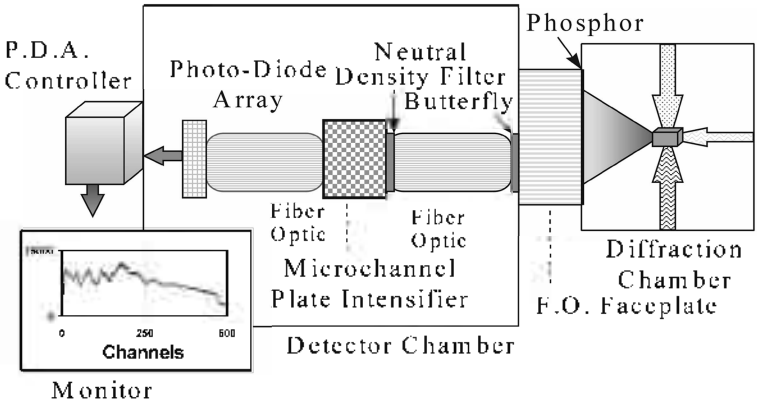

Fig. 4. Schematic Diagram of the Detector System for TRED.

cooled detector to reach its preset temperature of -37°C.

The electron beam is first visualized on the phosphor screen for alignment and focusing, and then placed inside the trap. After the initial alignment, the detector system is butted up against the phosphor screen, and then fine-tuned for the maximum diffraction signals. To align the PV, first the needle is placed on the center of the electron beam, then moved up. The laser pulses are first placed on the PV needle then moved slightly below to complete the intersection of electron pulses, molecular pulses and laser pulses.

RESULTS AND DISCUSSIONS

A) Investigation of Chlorotrifluoromethane ($CClF_3$) by GED/RT

A method for direct evaluation of equilibrium molecular geometries from GED/RT intensities was reported previously.[23,24] Based on a cumulant expansion for the molecular diffraction intensities, the method was applied to determine the equilibrium structures of sulfur hexafluoride SF_6[23] and selenium hexafluoride.[24] However, information on harmonic and anharmonic potential constants is required for the full cumulant analysis. The simplified CA as reported for SF_6 [25] allows for data refinements without the need for such extraneous information. The molecular parameters [r_e, λ_a, and γ_3, γ_4] were refined over a wide temperature range. The application of the new intensity expression to $CClF_3$ is important because it avoids the geometrically inconsistent r_a scheme of the traditional method commonly used in GED investigations. The simplified CA can be applied to equilibrium ensembles at elevated temperatures due to thermal heating or optical pumping, where the traditional method is inoperable.

The results of GED/RT investigations for $CClF_3$ comparing the simplified CA and traditional methods are presented. N_2 (99.998 %) was used as an internal standard for calibration of the GED/RT instrument. The mean equilibrium N≡N distance as determined from the calibration intensity data by excess CA is r_e = 109.74(1) pm. The calculated temperature-dependent distances r_a and r_g, mean amplitudes λ_a, λ_g, and phase shift parameter k agree well with the result of previous work [24].

The molecule $CClF_3$ displays a well resolved distribution of internuclear distances. This molecule has been the subject of three prior photographic electron diffraction studies[26,27]. The simplified CA analysis was applied to GED intensities of $CClF_3$ without spectroscopic information over the temperature range from 298K to 673K. The experimental and theoretical intensity curves for $CClF_3$ are compared in *Fig.* 5. The radial distribution curves are shown in *Fig.* 6. The molecular parameters at various temperatures of $CClF_3$ by simplified CA are presented in *Tables* 1~3.

The positions, r_{RD}, of the maximum of the radial distribution peaks (r_{RD} = 1.328 ± 0.002Å for C-F, 1.751±0.004 Å for C-Cl, and ∠ FCF = 108.6 ± 0.4°) were reported by Bartell in 1955. The thermal average distances r_a=1.3257(14) Å for C-F, 1.7489 (39) Å for C-Cl, and ∠ FCF = 108.6 ± 0.2° were

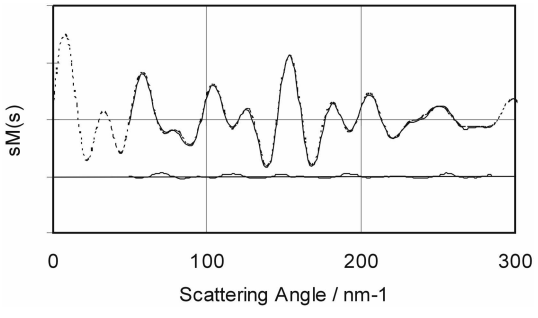

Fig. 5. Theoretical and Experimental Intensity Curves of CCIF3 at 298K.

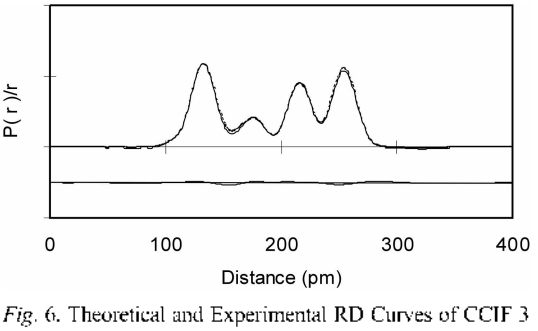

Fig. 6. Theoretical and Experimental RD Curves of CCIF 3 at 298K.

Table 1. The Equilibrium Molecular Parameters for C-F of $CCIF_3$ by Simplified CA

T/K	r_e	λ_a	γ_3	γ_4	R (%)
298	132.00 (2)	4.42 (1)	0.14448	-0.11634	4.6
373	132.01 (2)	4.43 (1)	0.14575	-0.11826	4.3
473	131.98 (2)	4.48 (1)	0.14670	-0.11970	4.7
573	132.02 (3)	4.65 (2)	0.15335	-0.12997	5.6
673	132.01 (3)	4.76 (2)	0.15777	-0.13699	6.4

The values of the parameters are given from analysis of averaged data sets at each temperature.
Uncertainties in parentheses for r_e (pm) and λ_e (pm) are 1σ.
The reproducibilities (R_f) are presented in percent.

Table 2. The Equilibrium Molecular Parameters of C-Cl for $CCIF_3$ by Simplified CA

T/K	r_e	λ_a	γ_3	γ_4
298	175.20(4)	4.50 (5)	0.14758	-0.12103
373	175.19(4)	4.76 (4)	0.15770	-0.13687
473	175.20(4)	5.06 (4)	0.16981	-0.15681
573	175.22(5)	5.28 (5)	0.17948	-0.17345
673	175.23(6)	5.44 (5)	0.18643	-0.18579

The values of the parameters are given from analysis of averaged data sets at each temperature.
Uncertainties in parentheses for r_e (pm) and λ_e (pm) are 1σ.

Table 3. The Equilibrium Molecular Parameters for F…F and F…Cl of $CCIF_3$ by Simplified CA

	F…F		F…Cl	
T/K	r_e	λ_a	r_e	λ_a
298	214.38	5.4(3)	253.22	6.4(2)
373	214.34	5.5(3)	253.30	6.8(2)
473	214.31	5.8(3)	253.34	7.3(2)
573	214.46	6.1(3)	253.39	7.7(2)
673	214.42	6.4(3)	253.36	8.2(3)

The values of the parameters are given from analysis of averaged data sets at each temperature.
Uncertainties in parentheses for λ_e (pm) are 1σ.

presented by Oberhamer in 1978. The microwave study of $CCIF_3$ was reported in 1952 [28] where the values of d_{CF} = 1.328 ± 0.005Å and d_{CCl} = 1.740 ± 0.0018Å were presented. The stretching and bending anharmonicity of $CCIF_3$ was studied by Bartell [29], but only the thermal average distances (r_a) at room temperature and bond asymmetry parameters were reported.

The molecular parameters of bonded C-F and C-Cl for $CCIF_3$ by simplified CA are shown in *Tables* 1~5; the mean equilibrium distances are r_e = 132.00 (2) pm and 175.20(3) pm, respectively. As expected, r_e is essentially independent of temperature as shown in *Figures* 7~8. As shown in *Table* 4 the temperature dependent mean distance is r_a = 132.64 (2) pm for C-F and r_a = 176.08(6) pm for C-Cl obtained at the room temperature by the traditional method. Also the temperature dependent vibrational amplitudes from the simplified CA are compared with those from the traditional method. The temperature dependent vibrational amplitudes λ_a of C-F, C-Cl, F…Cl, and F…F also increased and increases of the F…Cl amplitudes much larger than the others. The angles of Cl-C-F are 110.3 ± 0.2° and 110.0 ± 0.1° by the simplified CA and the traditional methods, respectively. Also, the increases of g_3 and the decreases of g_4 for both nonbonded F…F and Cl…F are much larger than for bonded C - F.

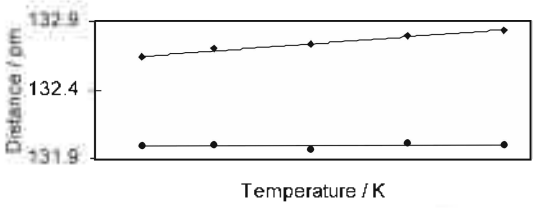

Fig. 7. The Comparison of re(●) and ra(◆) of C-F for CCIF3 Versus Temperatue.

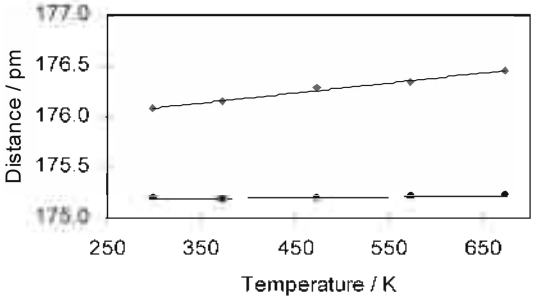

Fig. 8. The Comparison of re (●) and ra (◆) for C-Cl of CCIF3 Versus Temperature.

The data analyses of this study offer the opportunity to directly compare the results obtained by the traditional method and simplified CA. In the traditional method, κ asymmetry values are often assumed to be zero which leads to systematic shifts of the r_a distances. In view of this consideration and the results of this thesis, we expect that simplified

Table 4. The Thermal Averaged Molecular Parameters for C-F and C-Cl of $CClF_3$ by Traditional Method

	C - F		C - Cl	
T/K	r_a	λ_a	r_a	λ_a
298	132.64(2)	4.3(1)	176.08(6)	4.3(1)
373	132.70(3)	4.4(1)	176.15(7)	4.7(1)
473	132.73(5)	4.5(1)	176.28(5)	5.0(2)
573	132.79(5)	4.7(1)	176.34(7)	5.1(2)
673	132.83(4)	4.8(1)	176.45(7)	5.4(3)

The values of the parameters are given from analysis of averaged data sets at each temperature.
Uncertainties in parentheses for r_a (pm) and λ_a (pm) are 1σ.

Table 5. The Thermal Averaged Molecular Parameters of F...F and F...Cl for $CClF_3$ by Traditional Method

	F...F		F...Cl	
T/K	r_a	λ_a	r_a	λ_a
298	215.89(4)	5.4(1)	254.20(4)	6.6(1)
373	215.88(3)	5.6(1)	254.32(3)	6.9(1)
473	215.94(4)	5.8(1)	254.46(4)	7.4(1)
573	216.08(6)	6.1(1)	254.58(5)	7.9(1)
673	216.17(6)	6.5(1)	254.72(5)	8.4(1)

The values of the parameters are given from analysis of averaged data sets at each temperature.
Uncertainties in parentheses for r_a (pm) and λ_a (pm) are 1σ.

CA provides a more adequate account of the GED/RT experiments. When the simplified CA is applied directly to the GED/RT data, then the equilibrium molecular geometries are refined without information from spectroscopy. The simplified CA scheme may be applied to molecular ensembles at high temperatures and to IR-laser excited systems. Thus, we see its greatest value as establishing the much needed basis for structural kinetic studies of laser excited species by TRED. It will be interesting in the future to compare the results reported in this thesis for $CClF_3$ with those obtained from a full cumulant (excess) analysis including spectroscopic information on the molecular force field.

B) TRED Molecular Parameters of $CClF_3$

$CClF_3$ were studied under similar TRED experimental conditions at room temperature. Each frame of data (about 500 channels) contained the complete intensity pattern and required about 20 seconds integration time, and typically 20 to 50 frames were averaged to yield the data sets used for further processing. In a typical experiment, the data set of the molecule to be studied is recorded together with dark current (no gas present), and argon gas (atomic reference), as in GED/RT experiments.

The energy of the 500 fs laser pulses was amplified about 300 times with our modified amplifier. 10% of the amplifier output was directed to the electron chamber to make picosecond electron pulses. After focusing onto the photocathode, the spot diameter is about 2 mm. The other 90% provided the excitation source of molecular samples for the pump-probe experiment. The total temporal broadening (Δt_{FOT}) of the electron pulses was estimated to be ~20 ps.

Measurements of the temporal behavior of the molecular beam were conducted in two different configurations of the pulsed inlet. In the case of "free jet," the molecular pulse length was about 80 μs with argon or SF_6 gases. The measured pulse length is very close to the 110 μs pulse predicted by theoretical calculations.

The amplified femtosecond laser pulses yielded stronger diffraction signals than previous experiments for picosecond TRED. The use of the EF allows an increase in quality of diffraction intensities. The diffraction pattern from ~20 ps electron pulses was recorded by the PDA detector during exposure times of ~20 seconds. The total data acquisition time was about 7 minutes.

A lecture bottle of $CClF_3$ (Aldrich, 99%) was connected directly to the sample inlet of the pulsed valve of TRED to get the molecular structural parameters at room temperature. The ground state picosecond TRED patterns were recorded with 4000 electron pulses. The experimental ratio curve without any smoothing is presented in *Fig.* 9. The molecular intensity sM(s) and radial distribution curves are shown in *Fig.* 10 and 11, respectively. The structural parameters for $CClF_3$ with GED/RT and TRED are compared in *Tables* 6 and 7.

From our GED/RT, r_a for bonded C-F, C-Cl are 132.64(2) pm and 176.08 (6) pm, r_a for nonbonded F...F, F...Cl are 215.89(4) pm and 254.20(4) pm,

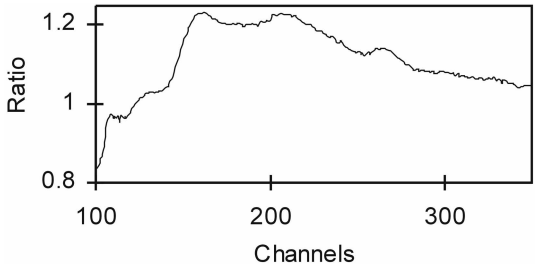

Fig. 9. TRED Experimental Ratio Curves of CCIF3 from 4,000 Electron pulses.

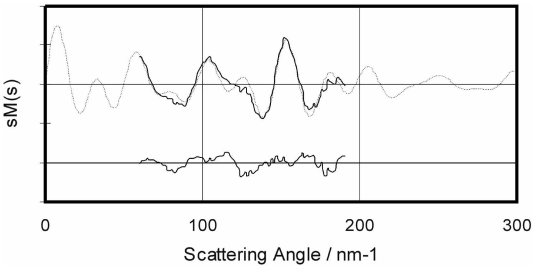

Fig. 10. Therotical (dot) and Experimental (solid) Intensity Curves of CCIF3 with TRED.

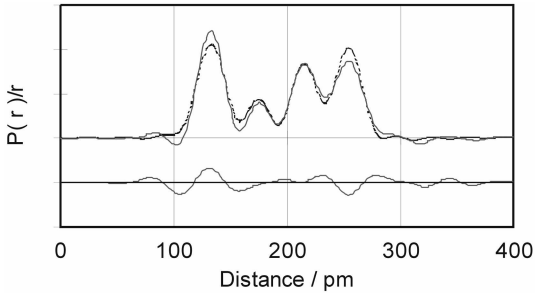

Fig. 11. Theoretical (dot) and Experimental (solid) RD Curves of CCIF3 with TRED.

and the angle of ∠ ClCF is 110.0 ± 0.1° by the traditional method. From the results of TRED experiments r_a for bonded C-F and C-Cl are 132.23(13) pm and 177.23(19) pm; r_a for nonbonded F…F and F…Cl are 215.90(12) pm and 254.05(14) pm, and the angle ∠ClCF is 109.5 ± 0.2°. The vibrational amplitudes $l_a$of C-F and F…F are summarized in *Tables* 6 and 7. When we compare the picosecond TRED results with those of GED/RT, the results of TRED are very close to those of GED/RT. In the future the TRED system can be used for studying transition states and photodissociation processes with picosecond time resolution.

Table 6. The Comparison of Molecular Parameters of C - F and C - Cl for $CClF_3$ with GED/RT and TRED by Traditional Method at 298K

	C - F		C - Cl	
	r_a	λ_a	r_a	λ_a
GED/RT	132.64(6)	4.3(3)	176.1(2)	4.3(3)
TRED	132.23(40)	4.7(9)	177.2(6)	5.5(3)

The values of the parameters (in pm) are given as obtained from analyses of averaged data. Uncertainties in parentheses for r_a and λ_a are 3σ.

Table 7. The Comparison of Molecular Parameters of F…F and F…Cl for $CClF_3$ with GED/RT and TRED by Traditional Method at 298K

	F…F		F…Cl	
	r_a	λ_a	r_a	λ_a
GED/RT	215.89(4)	5.4(1)	254.20(4)	6.6(1)
TRED	215.90(12)	6.6(1)	254.05(14)	10.3(4)

The values of the parameters (in pm) are given as obtained from analyses of averaged data. Uncertainties in parentheses for r_a and λ_a are 1σ.

CONCLUSIONS

The data analysis of $CClF_3$ has compared the results obtained by the traditional method and by simplified CA. The equilibrium molecular geometry for $CClF_3$ was determined directly from the GED/RT data without extraneous information from spectroscopy. When the simplified CA is applied directly to the GED/RT data, then the equilibrium molecular geometries are refined without information from spectroscopy. The simplified CA scheme can be applied to molecular ensembles at high temperatures and to IR-laser excited systems. Thus, we see its greatest value as establishing the much needed basis for structural kinetic studies of laser excited species by TRED. It will be interesting in the future to compare the results reported in this paper with those obtained from a full cumulant (excess) analysis including spectroscopic information on the molecular force field.

In this study, the TRED apparatus was tested and improved. The 500fs laser pulses are amplified, the total temporal broadening of the electron pulses is

estimated to be ~20 ps, current data collection has become routine in picosecond time resolution, collection times have decreased, and the TRED system is applied to study the molecular structures of ground state CCl_3 system in picosecond time domain.

REFERENCES

1. J. D. Ewbank, L. Schäfer, D. W. Paul, O. J. Benston, J. C. Lennox, *Rev. Sci. Instrum.*, **1984**, *55*, 1598.
2. a) J. D. Ewbank, L. Schäfer, D. W. Paul, D. L. Monts, W. L. Faust, *Rev. Sci. Instrum.*, **1986**, *57*, 967, b) L. Schäfer, J. D. Ewbank, *Acta Chem. Scand.*, **1988**, *A42*, 358, c) J. D. Ewbank, D. W. Paul, L. Schäfer, R. Bakhtiar, *Appl. Spectrosc.*, **1989**, *43*, 415.
3. V. P. Spiridonov, A. G. Gersikov, E. Z. Zasorin, B. S. Butayev, *Diffraction Studies on Non-Crystalline Substances*, I. Hargittai, W. J.Orville-Thomas, Eds., Arkademiai Kiado: Budapest, 1981.
4. A. A. Ischenko, J. D. Ewbank, L. Schäfer, *J. Phys. Chem.*, **1994**, *98*, 4287.
5. P. Maggard, A. A. Ischenko, V. A. Lobastov, L. Schäfer, J. D. Ewbank, *J. Phys. Chem.*, **1995**, *99*, 13115.
6. A. A. Ischenko, V. A. Lobastov, L. Schäfer, J. D. Ewbank, *J. Mol. Struct.*, **1996**, *377*, 261.
7. A. H. Zewail, *Femtochemistry; Vols. 1 and 2*, World Scientific, Singapore, Hong-Kong, **1994**.
8. A. A. Ischenko, V. V. Golubkov, V. P. Spiridonov, et al., *Appl. Phys.*, **1983**, B32, 161.
9. J. D. Ewbank, W. L. Faust, J. Y. Luo, et al., *Rev. Sci. Instrum.*, **1992**, *63*, 3352.
10. a) J. Cao, H. Ihee, and A. H. Zewail, *Chem. Phys. Lett.*, **1997**, *281*, 10. b) M. Dantus, S. B. Kim, J. C. Williamson, A. H. Zewail, *J. Phys. Chem.*, **1994**, *98*, 2782. c) J. C. Williamson and A. H. Zewail, *J. Phys. Chem.*, **1994**, *98*, 2766.
11. A. A. Ischenko, L. Schäfer, and J. D. Ewbank, *Time-Resolved Diffraction*, Edited by J. R. Helliwell and P. M. Rentzepis, Clarendon Press, Oxford, **1997**.
12. A. A. Ischenko, L. Schäfer, and J. D. Ewbank, *Tomography of theMolecular Quantum State by Time-Resolved Electron Diffraction*, Proc. SPIE **1999**, *3516*, 90.
13. J. Karle, in I. Hargittai and W. J. Orville-Thomas, Eds., *Diffraction Studies of Non-Crystalline Substances*, Akademiai Kiado, Budapest, **1981**.
14. A. A. Ischenko, V. P. Spiridonov, et al. *J. Mol. Struct.*, **1988**, *172*, 255-273.
15. A. A. Ischenko, V. V. Lobastov, L. Schäfer, J. D. Ewbank, *J. Mol. Struct.*, **1996**, *377*, 261-269.
16. J. L. Kuester, J. H. Mize, *Optimization Technique with FORTRAN*, McGraw-Hill, New York, **1973**.
17. A. A. Ischenko, J. D. Ewbank, L. Schäfer, *J. Phys. Chem.*, **1994**, *98*, 217.
18. J. D. Ewbank, D. W. Paul, L. Schäfer, *IR 100 Awards, Research and Development*, October, **1985**.
19. A. A. Ischenko, L. Schäfer, and J. D. Ewbank, *Time-Resolved Diffraction*, Edited by J. R. Helliwell and P. M. Rentzepis, Clarendon Press, Oxford, **1997**.
20. a). S. Szatmari and F. P. Schäfer, *Appl. Phys.*, 1988, B49, 305. b) S. Szatmari, G. Almasi, and P. Simon, *Appl. Phys.*, **1991**, B53, 82.
21. J.R. Pierce, *Theory and Design of Electron Beams*, Van Nostand, Princeton, NJ, **1954**.
22. W. R. Gentry and C. F. Giese, *Rev. Sci. Instrum.*, **1978**, *49*, 595.
23. A. A. Ischenko, L. Schäfer, and J. D. Ewbank, *Time-Resolved Diffraction*, Edited by J. R. Helliwell and P. M. Rentzepis, Clarendon Press, Oxford, 1997.
24. A. A. Ischenko, J. D. Ewbank and L. Schäfer, *J. Phys. Chem.*, **1994**, *98*, 4287.
25. P. Maggard, V. A. Lobastov, L. Schäfer, J. D. Ewbank, A. A. Ischenko, *J. Phys. Chem.*, **1995**, *99*, 13115.
26. A. A. Ischenko, V. A. Lobastov, L. Schäfer and J. D. Ewbank, *J. Mol. Struct.*, **1996**, *377*, 261.
27. L. S. Bartell and L. O. Brockway, *J. Chem. Phys.*, **1955**, *23*, 1860.
28. V. Typke, M. Dakkouri, H. Oberhammer, *J. Mol. Struct.*, **1978**, *44*, 85.
29. D. K. Coles, R. H. Hughes, *Phys. Rev.*, **1949**, *76*, 858.